Solar Cell Structure Defects and Cracks

Skarvada P.[a], Tomanek P.[b], Dallaeva D.[c]

Brno University of Technology, Faculty of Electrical Engineering

and Communication, Department of Physics

Technicka 8, 616 00 Brno, Czech Republic

[a] skarvada@feec.vutbr.cz, [b] tomanek@feec.vutbr.cz, [c] xdalla02@stud.feec.vutbr.cz

Keywords: silicon solar cell, bulk defects, edge defects, scanning probe microscopy, laser beam induced current.

Abstract. Photon emission from the reverse biased silicon solar cell samples was used for localization of defects. Light was detected in the wavelength range 350-800 nm. Laser beam induced current technique was used for crack localization and results were correlated with light emission. Defects that emit photons with mechanism different to avalanche breakdown were investigated in microscale using scanning electron microscopy. In the most of the defective areas structure damages uncovering the pn junction have been found.

Introduction

Producers of optoelectronic structures and devices are trying to improve quality of products, increase its efficiency and reliability, and at the same time to minimize production costs with contradictory effect on other parameters of devices. This trend can be clearly seen in photovoltaics. With miniaturization and on-set of devices with very fine structure, there is also the topical need of the new or improved characterization and diagnostic methods with very high spatial resolution. However, there are still many of problems in the material engineering related with understanding of effects of current devices but mainly cohere with devices development.

Electric measurement is the basic approach for semiconductor devices characterization. Electric testing can determine sample properties of optoelectronic devices, and roughly estimate the existence of defects, but the knowledge about the defect localization on the sample is hard to reach [1, 2]. Another common group of diagnostic methods are techniques based on luminescence [3]. Photoelectric measurements are the most common testing methods for optoelectronic devices, and are also very important for defects characterization. Nevertheless only microscopic study of defects can evidently revail their nature.

The most of the structure defects are created during processing steps such as cutting, deposition in high temperatures, metallization, etc. Thus there is a large variety of defects with different behavior and nature such as Schottky and ohmic shunts, edge shunts, cracks and dislocations. These defects provide parasitic recombination sites and affect devices parameters. Some of the recombination centers such as an avalanche breakdown region also emit light while the sample is in forward or reverse biased conditions [4].

Local avalanche breakdown which originate in the structure defect is one of the most numerous bulk defects in the silicon monocrystalline solar cells. These defects can be usually considered as small pits with diameter smaller than a few micrometers on the surface of the cell [5]. Pits affect current voltage characteristics and provide a light emission invisible range while the sample is in reverse

biased condition. Except defect resulting in impact ionization and avalanche breakdown [6], there are various defects exhibiting light emission in reverse bias but their nature is different [7].

Measurement techniques

Laser beam induced current. Laser beam induced current (LBIC) is a method used for localization of crack, scratches and shunts. The method is based on local optical excitation and measurement of amount of generated free carriers via short circuit current measured by transimpedance amplifier. By scanning of laser beam, the LBIC image can be acquired. Basically the external quantum efficiency is measured on selected wavelengths. Surface defects are better visualized with use of short wavelength lasers, while the substrate defects are better observable using longer wavelengths.

Light emission measurement. Sensitive CCD camera working in required wavelength range is the most often a detector used for this measurement. Alternatively, the photomultiplier tube in photon counting regime can be used for the detection of weak light emission signals. In this case the scanning optical probe has to been used. Used photomultiplier has the peak sensitivity in visible range (working wavelength range 350 nm to 800 nm). Sample is thermally stabilized and voltage bias is controlled by computer. The finest step of scanning optical probe is 25 μm.

Microscale defect characterization. For microscale defect characterization scanning electron microscope was used. Some defects are not observed in topography inhomogeneity. Thus for these defects scanning near-field optical microscope is a unique tool able to detect defect area. It allows the local measurement of optical properties with sub-wavelength resolution, light emission and surface topography measurement. Alternatively, it can be used for near-field optical beam induced current (n-OBIC) measurement [8].

Experimental

Investigated solar cell sample of monocrystalline silicon solar cell was measured using LBIC with used wavelength of 532 nm. Green light was selected to measure mainly near the surface external quantum efficiency. The top right edge of the sample was broken off. LBIC measurement revealed formation of the second crack (Fig. 1). Moreover small imperfection can be seen near the third top metallization contact (counted from bottom).

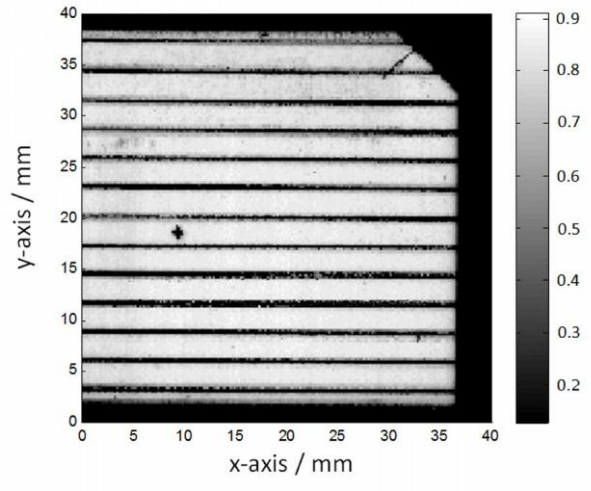

Fig.1. Normalized LBIC image of Sc3 sample, excitation laser wavelength λ = 532 nm, ambient temperature T = 303 K.

Light emission from the sample in the visible and near infrared range was measured while the sample was in reverse biased conditions U_r = -12.4 V. Light emission originated from sample edge is seen in Fig. 2. However, edges created by breaking have usually higher leakage resistance and lower light emission compared to saw processed border, therefore one light emission center can be identified in this figure. Several light emission centers can also be seen in the bulk of the sample. Bulk defects are structure defects for the most part, structure damages and in some cases top metallization defects.

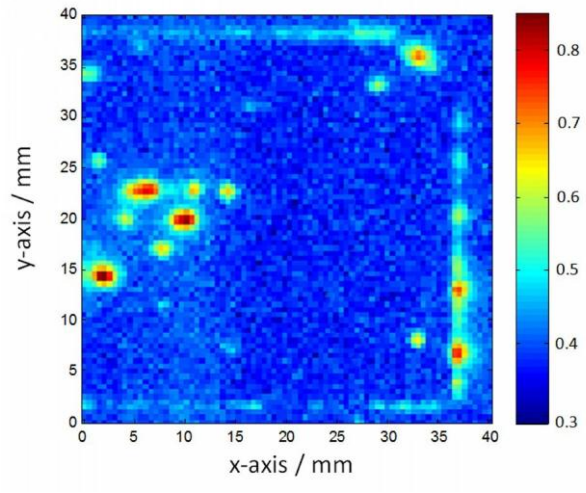

Fig.2. Normalized light emission map of Sc3 sample, measured wavelength range 350-800 nm, reverse bias of the sample U_r = -12.4 V, ambient temperature T = 303 K.

The matching of Figs. 1 and 2 is used for correlation of the light emission with sample top metallization, cracks and borders (Fig. 3). The most of bulk defects is caused by poorly created metal semiconductor contact in this sample. Parameters like annealing temperature and time were not optimized which results in leaky or shorted junctions under the grid lines [9].
Areas of interest were marked in the Fig. 3 as Area 1-4. Area 1 is the edge created by breaking with no photon emission. Except contact defects there is observable light emission from saw processed edges from the front side (area 2), crack (area 3) and structure damage (area 4).

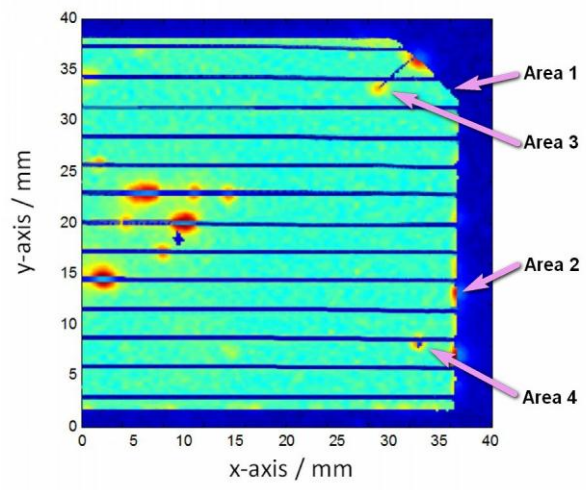

Fig.3. Combination of Figs 1 and 2 with marked areas 1-4 for further SEM investigation.

SEM micrograph of the solar cell sample edge created by breaking is shown in Fig. 4. Surface texture is not damaged hence the surface states are created only on the edges. Recombination activity of surface states is low and so the weak light and thermal emission can be measured. Amount of the light emission (area and intensity) can be considered as indirect indicator of the shunt conductivity regarding experimental results [10].

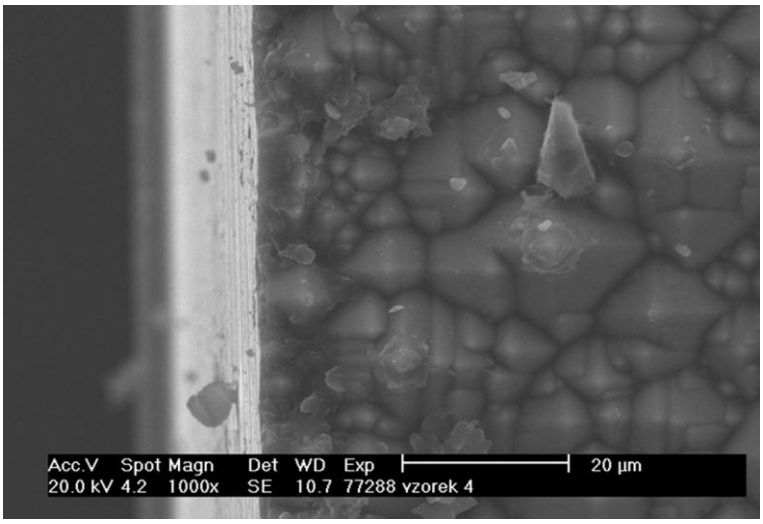

Fig.4. SEM micrograph of solar cell edge created by breaking (Area 1).

For edge processing several techniques are being currently used. Basic techniques are sawing and grinding, plasma etching and laser isolation. Besides the ability of techniques to isolate the edge of samples with *pn* junction created by diffusion process, there are also some advantages and disadvantages for the industrial use. Although the results of mechanical isolation are not bad (considering shunt resistance and efficiency), light emission from edges indicates some process-induced shunts. Damaged surface texture of saw processed edge is shown in Fig. 5.

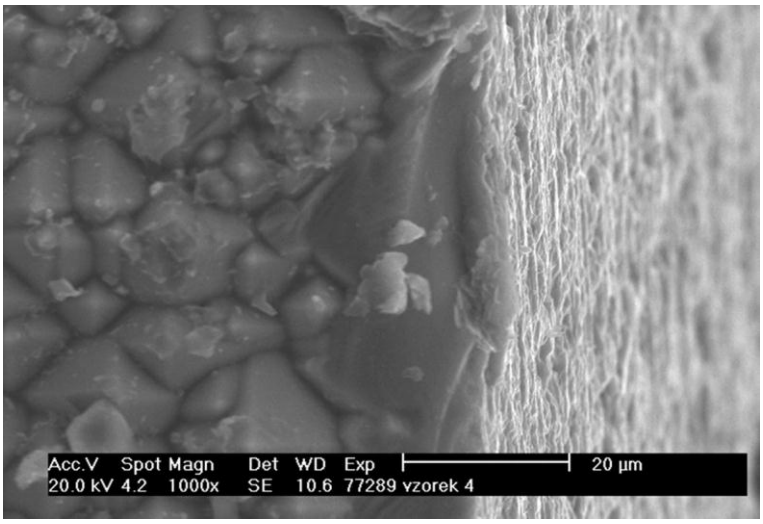

Fig.5. SEM micrograph of solar cell edge created by wire-saw from the front side (Area 2).

Mechanical damage of edge is not the only edge imperfection that can affects the cell parameters. More important defect is caused by poor isolation process. After the diffusion process that creates the *pn* junction, it is necessary to remove conductive semiconductor layer from the edges that shunting the *pn* junction. This is the reason why the edge isolation process is necessary. If the conductive edge is not properly removed, the shunt resistance will be low and it will reduce the efficiency of the cell. This situation is clearly observable in LBIC image (Fig. 6).

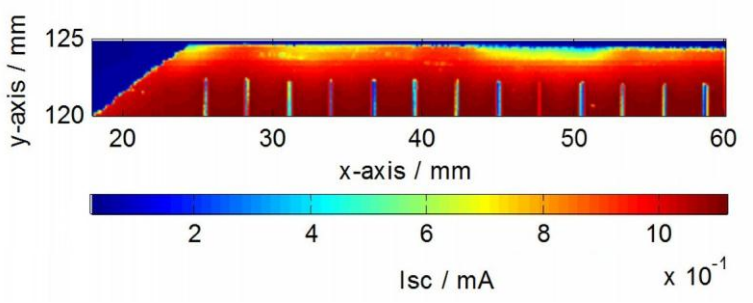

Fig.6. LBIC of poorly isolated edge of diffusion based solar cell.

Light emission (while the sample is reverse biased) from borders and structural damage has the same dependence on temperature - positive (Fig. 7) as we reported elsewhere [11]. LBIC image of area in the vicinity of the Spot 2 shows a presence of crystal crack that is evidently related to the photon emission. Positive dependence is considered to be internal field emission [12]. Thus the temperature growth causes the reverse current rising. Contrariwise, the negative temperature dependence of the photon emission (Spot 3) is caused by avalanche breakdown. The temperature growth increases the breakdown voltage and so it lowers a light emission.

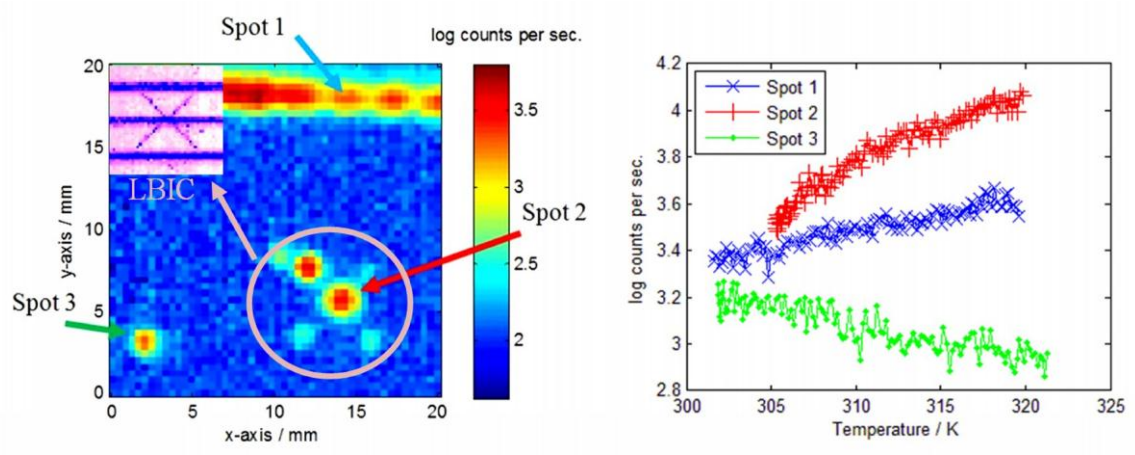

Fig.7. Light emission from sample with crack U_r = 24.0 V, T = 298 K (left), related light emission vs. temperature plot U_r = 24.0 V (right).

Some defects of like avalanche breakdown type cannot be localized using scanning electron microscope. This type of defects is shown in Fig. 8. Although there is no inhomogeneity on the surface, a local avalanche breakdown can be confirmed using electric and photon emission measurement at different temperatures.

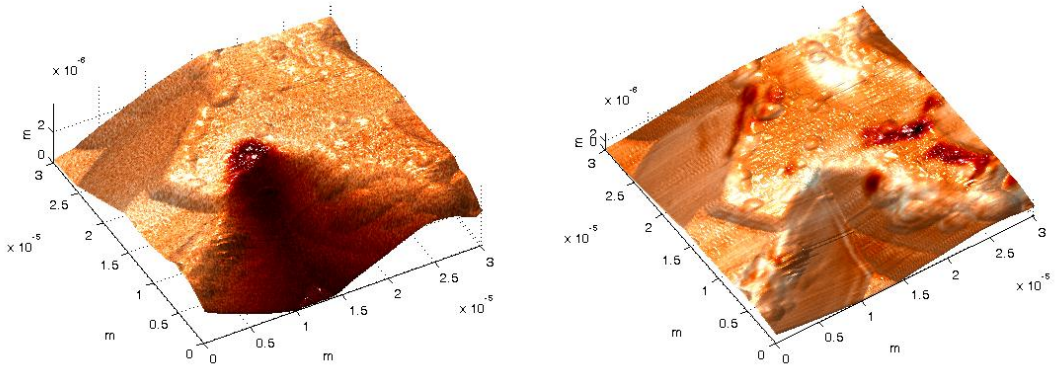

Fig.8. SNOM image of like avalanche breakdown type defect. Light emission shadow map Ur = 10 V (left), n-OBIC image of defect (right).

Regarding light emission temperature dependence, it was assumed that the mechanism of light emission is the same for the mechanical structure damage, cracks and edge emissions. The structural damage that uncovers the *pn* junction can be found on the edges of microcracks (Fig. 9).

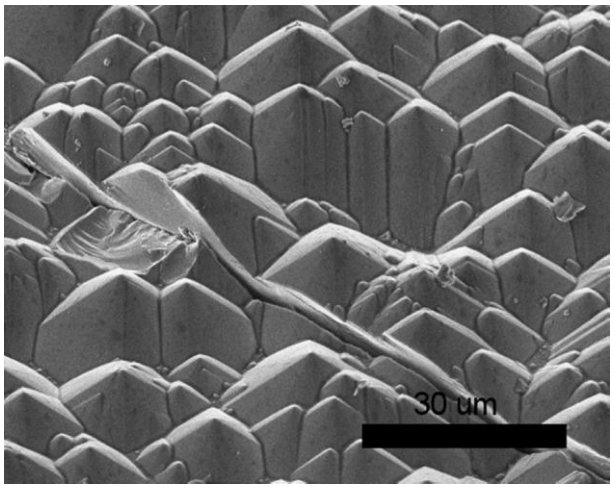

Fig.9. SEM micrograph of the sample microcrack (Area 3).

Structure damage resulting in photon emission in reverse biased condition is not only related to the crack and edge isolation process, but can be a product of surface scratching. LBIC image and SEM micrograph of the scratch near the top metallization is shown in Fig. 10. Except metal particles on the tops of the texture some minor damage can be found in the whole length of scratch.

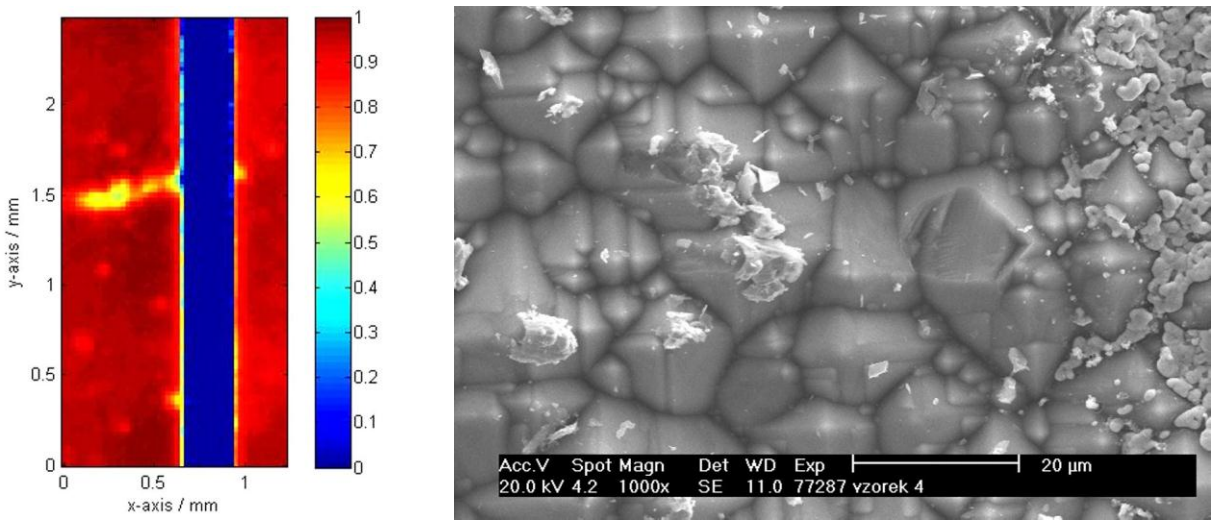

Fig.10. Normalized LBIC image of scratch (left), SEM micrograph of the damaged structure (Area 4 in Fig. 4) in the scratch (right).

Summary

We studied the surface structure of the solar cells with mechanical damages. Both microcracks and scratches showed localized photon emission when the solar cell was held in the reverse biased regime ($U_r > 10$ V). Light was detected in the wavelength range 350-800 nm and emitting spots were correlated with crack and scratches detected by LBIC. Cracks and scratches were localized also in microscale using scanning electron microscope. Similar structure damages uncovering *pn* junction for crack, borders and scratching have been found. This is most likely because in all cases the defects expose the pn junction and allow a creation of surface states.

Acknowledgement

This work has been supported by the GACR grant GAP102/10/2013, OPVK project CZ.1.07/2.3.00/09.0214, SIX research center project CZ.1.05/2.1.00/03.0072, and by Central European Institute of Technology CEITEC CZ.1.05/1.1.00/02.0068. These supports were gratefully acknowledged.

References

[1] P. Skarvada, P. Tomanek, L. Grmela and S. Smith: Sol. Energ. Mat. Sol. C., Vol. 94 (2010), p. 2358-2361.
[2] R. Macku, P. Koktavy, in: Phys. Status Solidi A, (2010) Vol. 207, DOI: 10.1002/pssa.201026206.
[3] P. Skarvada, L. Grmela, P. Tomanek: Key Eng. Mat., Vol. 465 (2011), p. 239-242.
[4] D. Kendig, G.B. Alers, A. Shakouri, in: 35th IEEE Phot. Spec. Conf. DOI 10.1109/PVSC.2010.5616109, (2010), p. 1733–1736.
[5] J. W. Bishop: Sol. Cells, Vol. 26 (1989), p. 335-349.
[6] P. Koktavy, M. Raska, P. Sadovsky, O. Krcal: in AIP Conf. Proc., Vol. 922 (2007), p. 141-144.
[7] L. Grmela, P. Skarvada, P. Tomanek, R. Macku, S. Smith: Sol. Energ. Mat. Sol. C., Vol. 96 (2012), p. 108-111.

[8] S. Smith, P. Zhang, T. Gessert, A. Mascarenhas: Appl. Phys. Lett., Vol. 85 (2004) p. 3854-3856.
[9] D. K. Schroder, D. L. Meier: IEEE T. Electron Dev. Vol. ED-31 (1984), p. 637-647.
[10] A. Hauser, G. Hahn, M. Spiegel, H. Feist, O. Breitenstein, J. P. Rakotoniaina, P. Fath, E. Bucher: in 17th European Photovoltaic Solar Energy Converence and Exhibition, Munich (2001).
[11] P. Skarvada, P. Tomanek, L. Grmela: in Proc. of SPIE, Vol. 8306 (2011), p. 1H1-1H6.
[12] A. G. Chynoweth and K. G. McKay: Phys. Rev., Vol. 106 (1957).